International Forum on Aeroelasticity and Structural Dynamics
IFASD 2019
9-13 June 2019, Savannah, Georgia, USA

ONERA-TYPE CORRECTIONS INTO THE UNSTEADY VORTEX LATTICE METHOD FOR DYNAMIC STALL REPRESENTATION

Carlos R. dos Santos[1], Flávio D. Marques[1], Haithem E. Taha[2]

[1]University of São Paulo
São Carlos, São Paulo 13566-590 Brazil
carlos.renan.santos@usp.br
fmarques@sc.usp.br

[2]University of California, Irvine
Irvine, California 92697 USA
hetaha@uci.edu

Keywords: dynamic stall, semi-empirical model, unsteady aerodynamics, panel method, finite wing

Abstract: Modeling of the dynamic stall is crucial for analyzes of aeroelastic systems that may attain high angles of attack in some operational regime. For two-dimensional studies, some methods have been developed in the last decades. Analyzes of helicopter blades and wind turbines, for example, frequently use the ONERA and the Beddoes-Leishman models. However, the modeling of dynamic stall in finite wings still lacks on fast and efficient models. In this sense, the present work proposes the development of a modified unsteady vortex lattice method (UVLM) considering an ONERA-based methodology to modify the loads assessed by the classical UVLM at each time step. By doing so, dynamic stall effects are captured using only the static lift curve and the empirical coefficients for the ONERA associated with the airfoils in the wing. Moreover, the difference between linear and stalled values for the lift coefficient in the static condition will be given through the Kirchhoff flow model. Results show good agreement between computational and experimental data, indicating that the proposed methodology can be employed in analyses of finite wings in which dynamic stall effects are relevant.

1 INTRODUCTION

At low angles of attack, aerodynamic loads of airfoils in the steady regime are usually classified as behaving linearly. As high angles of attack are attained, the flow separation induces nonlinearities in the loads, especially the lift reduction in the phenomenon known as stall. In unsteady cases, this sequence of events accounts for delay effects in both the pressure distribution and the flow separation over the airfoil. Moreover, the appearance and excursion of leading edge vortices are also relevant for the airfoil loading and all these events are sources of nonlinearities that must be considered during the dynamic stall [1].

As a consequence, the dynamic stall modeling remains a challenge. Even simulations of Reynolds Averaged Navier-Stokes equations may fail to represent the flow reattachment depending on the adopted turbulence method [2]. The use of discrete vortex methods was also proposed as an alternative for the assessment of aerodynamic characteristics of airfoils during dynamic stall [3]. However, the computational cost of such analyzes increases with the appearance of new vortices in the system. As alternatives of low computational cost, some

semi-empirical approaches were proposed for the prediction of aerodynamic loads during dynamic stall, such as the Beddoes-Leishman method [4] and the ONERA method [5]. Therefore, they depend on constants obtained from the fitting of experimental data.

In the case of the ONERA model, it was first developed to model aerodynamic loads during dynamic stall considering ordinary differential equations (ODE). One first-order ODE represents the linear regime and a second-order ODE emulates nonlinear effects that must be added to the linear term to deliver the total aerodynamic loads. The difference between linear and nonlinear static loads are used as input to the second-order ODE, thereby representing a source of nonlinearity to the system [5]. The ONERA model was employed to aeroelastic analyses of wind turbines blades [6], identification of limit cycle oscillations and chaotic behaviors of elastic mounted airfoils [7] and also for representation of dynamic stall loads at low wind speeds [8].

However, as observed in [9], the output of the first-order ODE responsible for the representation of linear loads does not follow the exact response given by the Wagner method. In addition, as shown in [10], the first-order ODE adopted by the ONERA model does not compute the same lift deficiency function found by [11] in relation to the circulatory lift. As consequence, the authors proposed the substitution of the first-order ODE by a second-order ODE.

In fact, the potential flow theory is a convenient approach to the assessment of aerodynamic loads at low Mach numbers. References [11], [12] and [13] are classical examples of methodologies where the potential flow was assumed for the calculation of aerodynamic loads during harmonic oscillations. Recently, reference [14] presented a compact state-space representation of unsteady aerodynamics based on the potential flow theory and considering the quasi-steady circulation as input for the model. Such methodology is very appropriate for simulations of two-dimensional aerodynamics considering arbitrary motions of the airfoil. In addition, [15] modified the potential flow theory by including viscous effects through the triple deck theory as a replacement of the Kutta condition. Such replacement also affects the calculation of the flutter velocity as a function of the Reynolds number [16].

Linear aerodynamics due to arbitrary motions at low wind speeds are also well represented by using panel methods with a distribution of vortices in two-dimensional cases or vortex rings in three-dimensional cases [17]. The wake is also represented by vortices or vortex rings that are shed at each time step and the non-penetration boundary condition is employed for the determination of the bond vorticity.

In this sense, the present work uses the capabilities of the UVLM to compute linear aerodynamic loads at low wind speeds. Dynamic stall nonlinearities are assessed through the second-order ODE of the ONERA method whose additional circulations are added to the circulations computed by the classical UVLM at each time step. The differences between linear and nonlinear static lift are modeled by the Kirchhoff flow. To the best of authors' knowledge this is the first time that a methodology for coupling the UVLM and the ONERA method is proposed.

2 METHODOLOGY

In the classic UVLM [17], the aerodynamic surface and its wake are divided into panels, such as illustrated in Figure 1. One vortex ring is associated with each panel and, considering the no-penetration boundary condition, the value of each circulation is assessed through the solution of a system of equations in the form:

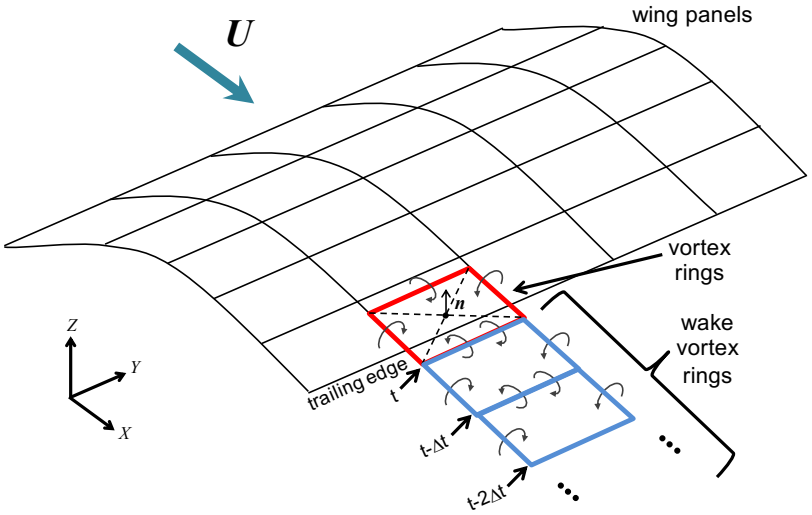

Figure 1: Discretization in the UVLM.

$$\begin{pmatrix} a_{1,1} & a_{1,2} & \dots & a_{1,K} \\ a_{2,1} & a_{2,2} & \dots & a_{2,K} \\ \vdots & \vdots & \ddots & \vdots \\ a_{K,1} & a_{K,2} & \dots & a_{K,K} \end{pmatrix} \begin{Bmatrix} \Gamma_1 \\ \Gamma_2 \\ \vdots \\ \Gamma_K \end{Bmatrix} = - \begin{Bmatrix} \mathbf{V}_1 \cdot \mathbf{n}_1 \\ \mathbf{V}_2 \cdot \mathbf{n}_2 \\ \vdots \\ \mathbf{V}_K \cdot \mathbf{n}_K \end{Bmatrix} , \tag{1}$$

where $a_{i,j}$ are aerodynamic influence coefficients, Γ_i is the circulation of each panel, and $\mathbf{V} \cdot \mathbf{n}_i$ denotes the normal velocity at each panel, including velocities induced by the wake.

After determining the values of Γ_i, the resultant force in each panel can be assessed from the unsteady Kutta-Joukowski theorem accordingly to [18]:

$$\mathbf{F} = \rho \hat{\Gamma} (\mathbf{U} \times \delta \mathbf{l}) + \rho c \frac{d\hat{\Gamma}}{dt} \frac{1}{U} (\mathbf{U} \times \delta \mathbf{l}) , \tag{2}$$

being ρ the air density, c the local chord length, $\mathbf{U}$ the freestream velocity and $\hat{\Gamma}$ the sum of circulations around a segment $\delta \mathbf{l}$.

On the other hand, the ONERA method for dynamic stall describes the dynamics of aerodynamic loads for two-dimensional sections by a set of differential equations. In the extended model proposed by [5] and modified by [19], the circulations composing the total lift are represented by:

$$\dot{\Gamma}_a + \lambda \left(\frac{2U}{c} \right) \Gamma_a = \lambda \left(\frac{2U}{c} \right) \frac{\partial C_l}{\partial \alpha} W_0 + \lambda \left(\frac{2U}{c} \right) W_1 + \left(\theta \frac{\partial C_l}{\partial \alpha} + \mu \right) \dot{W}_0 + \theta \sigma \dot{W}_1 , \tag{3}$$

and

$$\ddot{\Gamma}_b + a \left(\frac{2U}{c} \right) \dot{\Gamma}_b + r \left(\frac{2U}{c} \right)^2 \Gamma_b = -r \left[\left(\frac{2U}{c} \right)^2 U \Delta C_l + e \left(\frac{2U}{c} \right) \Delta \dot{C}_l \right] , \tag{4}$$

where λ, θ, μ, σ, a, r and e are semi-empirical parameters, W_0 and W_1 are associated with induced speeds, α is the local angle of attack and ΔC_l is the difference between the linear and nonlinear static curves for lift as function of the angle of attack. Then, the lift is calculated as a function of the circulations Γ_a and Γ_b.

Equation (3) represents linear loads and depends on four semi-empirical parameters. However, for low wind speeds, the potential flow theory is a convenient way to predict linear aerodynamic loads without the needing of semi-empirical parameters. Therefore, in the present work, Eq. (3) will be replaced by the loads given through the UVLM. Moreover, three-dimensional effects are properly reproduced by the UVLM, which allows the extension of dynamic stall analyses to finite wings.

On the other hand, Eq. (4) represents an additional circulation to the system and models dynamic stall nonlinearities. It is worth to note that the expressions in Eq. (3) and (4) are independent from each other. However, from the Beddoes-Leishman model for dynamic stall [20] important links between linear and nonlinear loads during dynamic stall are observed, such as the delay in the pressure distribution, the dynamic stall onset and the assessment of loads considering flow separation. Here, some of these effects are included in the ONERA model. Firstly, a lagged value for C_l, C_l^d is defined following the first order equation proposed by [20] for each strip j in the chordwise direction:

$$\dot{C}_{L_j}^d = \left(\frac{U}{b}\right) \frac{-C_{L_j}^d + C_{L_j}^{UVLM}}{T_p} \ , \tag{5}$$

where T_p is a empirical constant and C_L^{UVLM} is the value of C_L given by the UVLM for each strip.

From the value of $C_{L_j}^d$ an effective angle of attack, $\hat{\alpha}_j$, can be defined for each strip in the UVLM. Then, $\Delta C_{l_j} = \Delta C_{l_j}(\hat{\alpha}_j)$ is defined and the Kirchhoff's flow model [21] is employed to determine its value according to:

$$\Delta C_{l_j}(\hat{\alpha}_j) = 2\pi\hat{\alpha}_j \left\{1 - 0.25[1 + \sqrt{f(\hat{\alpha}_j)}]^2\right\} \ , \tag{6}$$

being f the portion of the airfoil where the flow remains attached. [20] offer an empirical representation of this parameter for NACA airfoils given by:

$$f(\hat{\alpha}_j) = \begin{cases} 1 - 0.3e^{\frac{|\hat{\alpha}_j| - \alpha_1}{s_1}} & \text{if } |\hat{\alpha}_j| \leq \alpha_1 \\ 0.04 - 0.66e^{\frac{\alpha_1 - |\hat{\alpha}_j|}{s_2}} & \text{if } |\hat{\alpha}_j| > \alpha_1 \end{cases} \ , \tag{7}$$

where α_1 is an angle defined when $f = 0.7$, usually near the stall angle, and s_1 and s_2 are constants defined empirically.

Finally, with the value of ΔC_{l_j} the circulation Γ_{b_j} can be determined for each strip and the final lift coefficient for each strip can be computed as:

$$C_{L_j} = C_{L_j}^{UVLM} + \frac{\Gamma_{b_j}}{U} \ . \tag{8}$$

3 RESULTS

Before three-dimensional analyses, the ONERA model was analysed as its capabilities on predicting the lift force under dynamic stall effects for two-dimensional airfoils. The method presented here replaces linear loading by the Theodorsen method and also includes the calculation

of ΔC_l as given by Equation (6). The case of study considers a NACA 0012 with chord 0.61 m at $U = 12.24$ m/s. The low wind speed selected for this test emulates the aerodynamic regime considered during three-dimensional analyses. The airfoil undergoes pitching oscillations according to $\alpha(t) = 14.65° + 14.04° \sin(2kUt/c)$, being $k = 0.104$ the reduced frequency of oscillation. Figure 2 compares the time history of the lift coefficient computed by the ONERA model with the results from the Beddoes-Leishman model [22] and experimental data from [23]. The time is nondimensionalized by $T = \pi c/(kU)$. For the NACA 0012, the values of $\alpha_1 = 15.5°$, $s_1 = 3$ and $s_2 = 2.3$ are adopted as in [22]. The parameters for Equation (4) in the ONERA model were set as $a = 0.18$, $e = 0.16 - \Delta C_l^2$ and $r = (0.1 + 0.15\Delta C_l^2)^2$ for a better matching between experimental and computational results. The parameter $T_p = 1.7$ was selected according to [22] and [24].

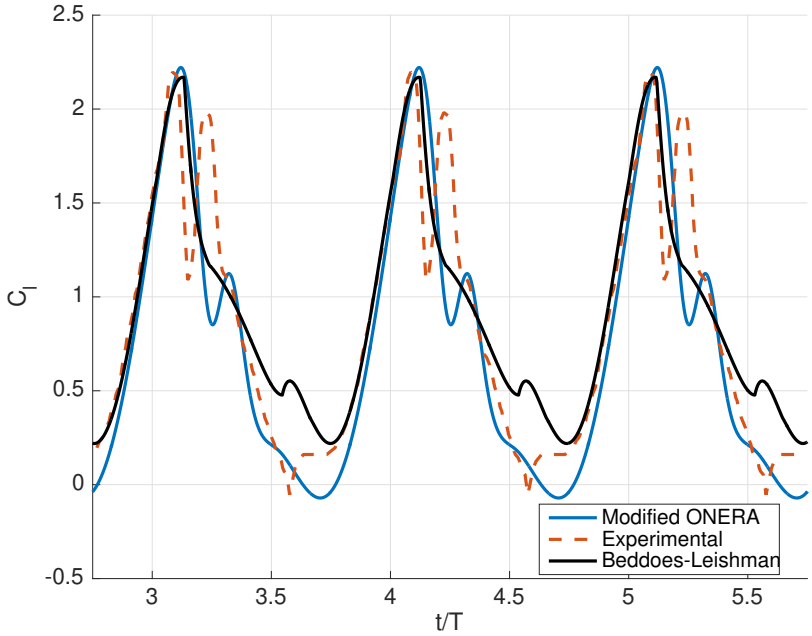

Figure 2: Comparison between ONERA and Beddoes-Leishman methods against experimental data.

The maximum lift calculated by the ONERA method and by the Beddoes-Leishman model are almost the same. However, it is extensively known that the Beddoes-Leishman method fails on capturing the loads during the flow reattachment [22]. Such problem is visible in the results presented in Figure 2. However, this limitation is not observed in the ONERA model. Moreover, the method was able to indicate the existence of a secondary peak in the lift after the stall, as observed in the experimental data. Therefore, the method can be considered an appropriate tool for lift prediction under dynamic stall effects at low wind speeds.

On the other hand, two options of UVLM can be considered for the simulation of linear loads: with a free-wake being deformed by all the potential velocities in the system; or a non-deforming wake, shed according to the freestream speed. Both approaches were compared and the resulting lift coefficients are compared in Figure 4. A rectangular wing, as illustrated in Figure 3, with aspect ratio $AR = 10$, $c = 0.305$ m at $U = 46.64$ m/s and undergoing pitching oscillations according to $\alpha(t) = 14.65° + 14.04° \sin(2kUt/c)$ was analyzed, being $k = 0.196$. This is the most critical case used for the validation of the presented three-dimensional model. The wing was divided in 30 panels in the span direction and 15 panels in the chord direction. The time step of the simulations was selected as 10^{-3} s. The maximum difference in the lift coefficient considering or not wake deformation is 0.4%. However, the computational time required for the

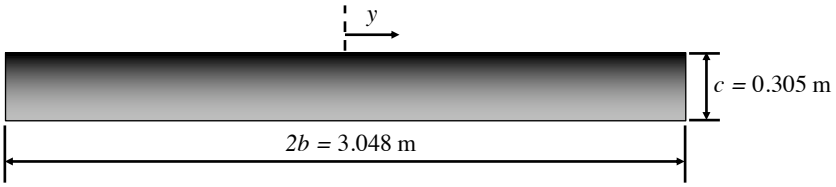

Figure 3: Schematic of the finite wing considered in this study.

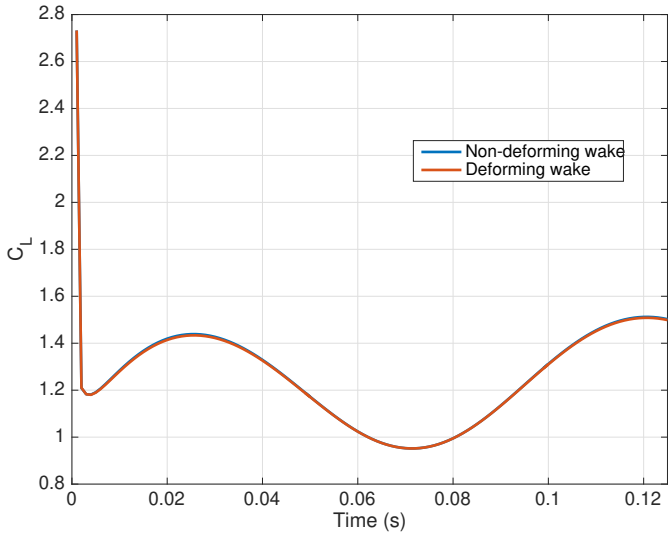

Figure 4: Comparison between the lift coefficient from the UVLM accounting or not for wake deformation.

simulation of 125 time steps considering a deforming wake was 266.3 s, while the simulation without wake deformation took 31.5 s. Both simulations were performed in a laptop with a 2.2 GHz Intel Core i7 processor. This result is in accordance with [25] that also observed that the computation of a free-wake does not improve the results in the UVLM considering angles of attack up to 8°. The same is valid for the high angles of attack in the present study. As consequence, the UVLM without wake deformation is selected for the analyzes in this work due to the lower computational time required.

A third investigation prior to the analyses of dynamic stall with the three-dimensional method addresses the mesh convergence in the UVLM method. Table 1 compares the difference between the value of maximum C_l computed by the UVLM with different grids in relation to the value computed using 100 panels in the span direction and 15 panels in the chord direction. As expected, this difference decreases as the number of panels increases, but also the computational cost increases with this refinement. Therefore, a grid with 30 spanwise panels and 15 chordwise panels was considered adequate for the analyses with a difference of 1.29% in relation to the most refined grid.

Table 1: Difference in the value of maximum C_l in relation to a grid with 100×15 panels (%)

	Chordwise panels			
Spanwise panels	5	10	15	20
10	4.73	4.71	4.31	3.91
20	2.54	2.51	2.13	1.74
30	1.69	1.66	**1.29**	0.90

Finally, results from the three-dimensional method for dynamic stall were compared with those

found in [26] for the rectangular wing illustrated in Figure 3 with airfoil NACA 0015. For this airfoil, the parameters $\alpha_1 = 13°$, $s_1 = 2°$, $s_2 = 2.3°$ and $T_p = 1.7$ were observed. The parameters for the ONERA model were kept the same as set for the two-dimensional study. In all the analyses the wind speed is kept at $U = 46.64$ m/s and the pitching oscillations are described by $\alpha(t) \approx 15.19° + 4.12° \sin(2kUt/c)$. Figure 5 shows the lift coefficient as function of the angle of attack for different reduced frequencies and at two positions of the span (considering the origin of the coordinates system at the middle of the span): $y/b = 0.25$ and $y/b = 0.5$. The selected positions are those with the most observable hysteresis due to dynamic stall effects. The graphics also compare the results with the output from the two-dimensional ONERA model considering the same empirical constants for Equation (4) and the Theodorsen model to predict linear loads.

Even at low reduced frequencies, dynamic stall effects are intense in the sections of the wing being examined. Especially for $y/b = 0.50$ (*c.f.* Figure 5(b)) the model indicated with good precision the maximum lift coefficient, which occurs at an angle of attack around 17°. However, the two-dimensional model predicts a lower dynamic stall angle and a higher maximum lift coefficient, which illustrates the importance of using a three-dimensional model to analyze the dynamic stall behavior of three-dimensional wings instead of a two-dimensional model only. If the reduced frequency is increased to $k = 0.098$, the maximum lift coefficient is attained at the maximum angle of attack during the motion. A similar behavior is observed for $y/b = 0.25$ (*c.f.* Figure 5(c)) and again for $y/b = 0.50$ (*c.f.* Figure 5(d)) the aerodynamic coefficients calculated through the three-dimensional method are closer to the experimental values. In these cases, the two-dimensional model approaches the experimental data while the angle of attack is decreasing, but the maximum lift coefficient is still over-predicted and the angle of dynamic stall is underestimated.

For cases at $k = 0.196$, the prediction of the lift coefficient at $y/b = 0.25$ (*c.f.* Figure 5(e)) presents good agreement with experimental data and at $y/b = 0.50$ (*c.f.* Figure 5(f)) the dynamics of the aerodynamic loading is replicated despite of some underestimation in the maximum lift coefficient and some overestimation of this coefficient at the lower angles of attack. However, the difference between results from the three-dimensional model and the two-dimensional model are huge at this reduced frequency. In fact, the coupling between a two-dimensional model for dynamic stall considering only parameters calibrated based on airfoil data with the UVLM is able to capture the main features of dynamic stall loading, thereby allowing its use as a reduced order model to be applied in aeroelastic analyzes.

4 CONCLUSIONS

This work described and validated a three-dimensional methodology for calculations of the lift coefficient of finite wings under dynamic stall effects. The model considers the UVLM for calculations of linear loads that will be corrected by an ONERA-type equation for each strip in the UVLM grid. The angle used for computation of the difference between the linear and nonlinear lift in the steady case is lagged following the approach presented in the Beddoes-Leishman model. Analyses regarding only UVLM capabilities indicated that for pitching oscillations of a rectangular wing, the presence of a free-wake does not modify the results despite of the considerable increasing in the computational cost. Finally, results from the complete three-dimensional methodology indicated that the use of the UVLM as a replacement for the linear loading in the ONERA method is an appropriate choice to account for three-dimensional effects in dynamic stall requiring only airfoil data.

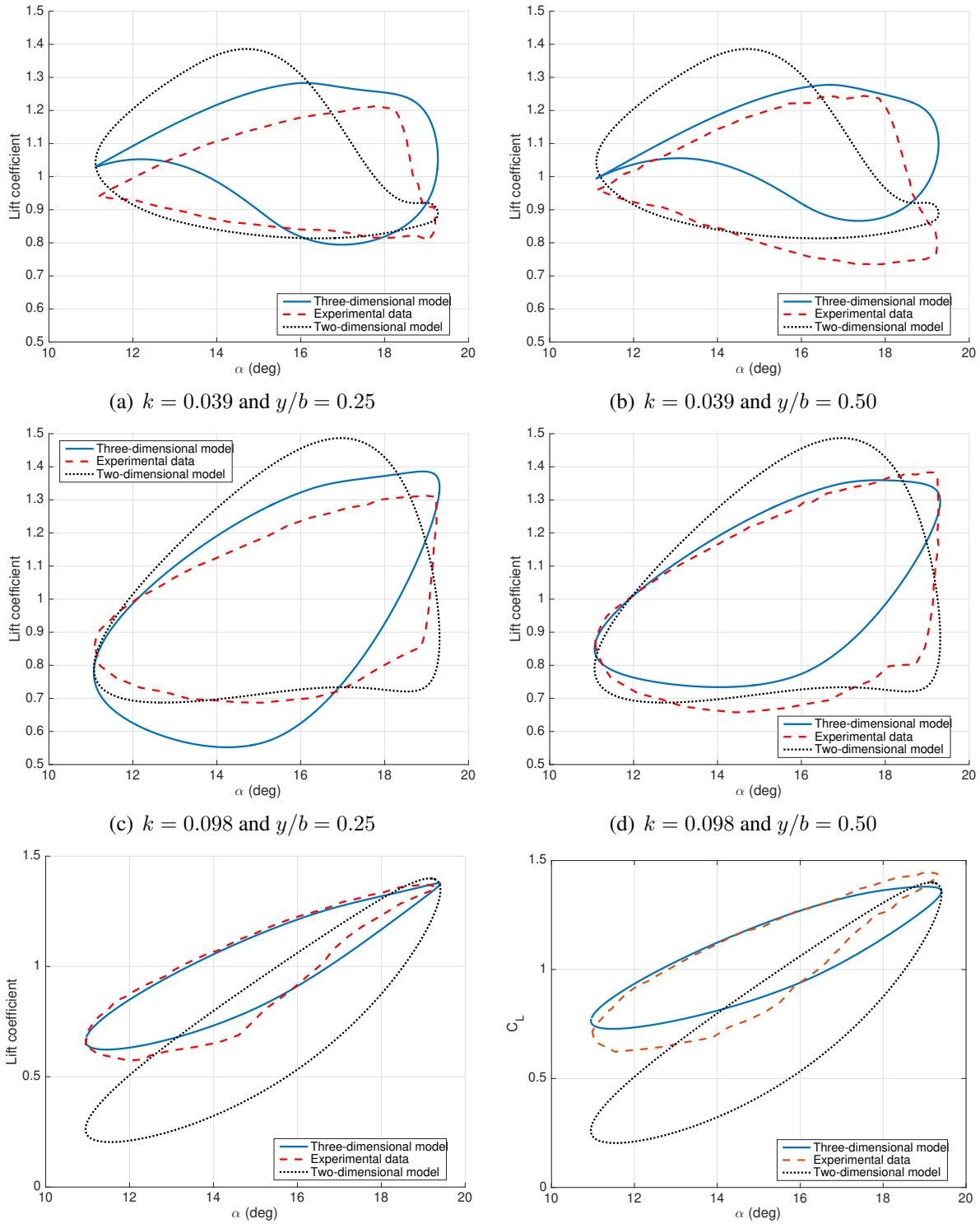

(a) $k = 0.039$ and $y/b = 0.25$

(b) $k = 0.039$ and $y/b = 0.50$

(c) $k = 0.098$ and $y/b = 0.25$

(d) $k = 0.098$ and $y/b = 0.50$

(e) $k = 0.196$ and $y/b = 0.25$

(f) $k = 0.196$ and $y/b = 0.50$

Figure 5: Comparison of the three-dimensional model against experimental data.

5 ACKNOWLEDGEMENTS

The first and the second authors acknowledge the sponsorship of: grants #2018/05247-8 and #2017/02926-9, São Paulo Research Foundation (FAPESP) and grant #307658/2016-3, National Council for Scientific and Technological Development (CNPq).

6 REFERENCES

[1] McCroskey, W. J. (1982). Unsteady airfoils. *Annual Review of Fluid Mechanics*, 14, 285–311.

[2] Wang, S., Ingham, D. B., Ma, L., et al. (2010). Numerical investigations on dynamic stall of low reynolds number flow around oscillating airfoils. *Computers & Fluids*, 39(9), 1529–1541.

[3] Ramesh, K., Murua, J., and Gopalarathnam, A. (2015). Limit-cycle oscillations in unsteady flows dominated by intermittent leading-edge vortex shedding. *Journal of Fluids and Structures*, 55, 84–105.

[4] Leishman, J. G. and Beddoes, T. S. (1986). A generalised model for airfoil unsteady aerodynamic behaviour and dynamic stall using the indicial method. In *Proceedings of the 42nd Annual forum of the American Helicopter Society*. Washington DC, pp. 243–265.

[5] Petot, D. (1989). Differential equation modeling of dynamic stall. *La Recherche Aerospatiale(English Edition)*, (5), 59–72.

[6] Shi, L., Riziotis, V., Voutsinas, S., et al. (2014). A consistent vortex model for the aerodynamic analysis of vertical axis wind turbines. *Journal of Wind Engineering and Industrial Aerodynamics*, 135, 57–69.

[7] Sarkar, S. and Bijl, H. (2008). Nonlinear aeroelastic behavior of an oscillating airfoil during stall-induced vibration. *Journal of Fluids and Structures*, 24(6), 757–777.

[8] Dunn, P. and Dugundji, J. (1992). Nonlinear stall flutter and divergence analysis of cantilevered graphite/epoxy wings. *AIAA journal*, 30(1), 153–162.

[9] Peters, D. A. (1985). Toward a unified lift model for use in rotor blade stability analyses. *Journal of the American Helicopter Society*, 30(3), 32–42.

[10] Laxman, V. and Venkatesan, C. (2007). Chaotic response of an airfoil due to aeroelastic coupling and dynamic stall. *AIAA journal*, 45(1), 271–280.

[11] Theodorsen, T. (1935). General theory of aerodynamic instability and the mechanism of flutter. NACA Rep. 496.

[12] Kármán, T. and Sears, W. R. (1938). Airfoil theory for non-uniform motion. *Journal of the Aeronautical Sciences*, 5(10), 379–390.

[13] Kussner, H. and Schwartz, I. (1941). The oscillating wing with aerodynamically balanced elevator. NACA T.M. 991.

[14] Taha, H. E., Hajj, M. R., and Beran, P. S. (2014). State-space representation of the unsteady aerodynamics of flapping flight. *Aerospace Science and Technology*, 34, 1–11.

[15] Taha, H. and Rezaei, A. S. (2019). Viscous extension of potential-flow unsteady aerodynamics: the lift frequency response problem. *Journal of Fluid Mechanics*, 868, 141–175.

[16] Taha, H. E. and Rezaei, A. S. (2019). Effect of viscous unsteady aerodynamics on flutter calculation. In *AIAA Scitech 2019 Forum*. p. 2036.

[17] Katz, J. and Plotkin, A. (2001). *Low-speed aerodynamics*, vol. 13. New York: Cambridge University Press.

[18] Simpson, R. J., Palacios, R., and Murua, J. (2013). Induced-drag calculations in the unsteady vortex lattice method. *AIAA journal*, 51(7), 1775–1779.

[19] Modarres, R., Peters, D. A., and Gaskill, J. (2016). Dynamic stall model with circulation pulse and static hysteresis for naca 0012 and vr-12 airfoils. *Journal of the American Helicopter Society*, 61(3), 1–10.

[20] Leishman, J. G. and Beddoes, T. S. (1989). A semi-empirical model for dynamic stall. *Journal of the American Helicopter Society*, 34, 3–17.

[21] Thwaites, B. (1960). *Incompressible aerodynamics*. Oxford: Clarendon Press.

[22] dos Santos, C. R., Marques, F. D., and Hajj, M. R. (2019). The effects of structural and aerodynamic nonlinearities on the energy harvesting from airfoil stall-induced oscillations. *Journal of Vibration and Control*.

[23] McAlister, K. W., Pucci, S. L., McCroskey, W. J., et al. (1982). An experimental study of dynamic stall on advanced airfoil sections – Volume 2: pressure and force data. Tech. rep., NASA and US Army Aviation Research and Development Command, Moffett Field. Technical memorandum, NASA-TM-84245; USAAVRADCOM TR-82-A-8.

[24] Dos Santos, C. R., Da Silva, M. M., and Marques, F. D. (2019). Optimization of energy harvesting from stall-induced oscillations using the multidimensional kriging metamodel. *Journal of Computational and Nonlinear Dynamics*.

[25] Lambert, T. (2015). *Modeling of aerodynamic forces in flapping flight with the Unsteady Vortex Lattice Method*. Ph.D. thesis, Universite de Liege - Belgique.

[26] Piziali, R. (1994). 2-d and 3-d oscillating wing aerodynamics for a range of angles of attack including stall. NASA T.M. 4632.

COPYRIGHT STATEMENT